Universal signatures of transposable element compartmentalization across eukaryotic genes

Landen Gozashti[1*] and Russell Corbett-Detig[2*]

[1] Department of Organismic & Evolutionary Biology, Department of Molecular & Cellular Biology, and Museum of Comparative Zoology, Harvard University, 16 Divinity Avenue, Cambridge, MA, USA

[2] Department of Biomolecular Engineering and Genomics Institute, University of California Santa Cruz, Santa Cruz, CA, USA

[*]lgozashti@g.harvard.edu, russcd@gmail.com

Abstract

The evolutionary mechanisms shaping the origins of genome architecture remain poorly understood but can now be assessed with unprecedented power due to the abundance of genome assemblies spanning phylogenetic diversity. Transposable elements (TEs) are a rich source of large-effect mutations since they directly and indirectly drive genomic structural variation and changes in gene expression. Here, we demonstrate universal patterns of TE compartmentalization across eukaryotic genomes spanning ~1.7 billion years of evolution, in which TEs colocalize with gene families under strong predicted selective pressure for dynamic evolution and involved in specific functions. For non-pathogenic species these genes represent families involved in defense, sensory perception and environmental interaction, whereas for pathogenic species, TE-compartmentalized genes are highly enriched for pathogenic functions. Many TE-compartmentalized gene families display signatures of positive selection at the molecular level. Furthermore, TE-compartmentalized genes exhibit an excess of high-frequency alleles for polymorphic TE insertions in fruit fly populations. We postulate that these patterns reflect selection for adaptive TE insertions as well as TE-associated structural variants. This process may drive the emergence of a shared TE-compartmentalized genome architecture across diverse eukaryotic lineages.

Main

The origins of eukaryotic genome architecture remain largely obscure. However, the breadth of annotated genome assemblies spanning a large portion of eukaryotic diversity now makes it possible to identify factors that shape genome evolution [1–3]. Transposable elements (TEs) are ubiquitous parasitic genetic elements capable of mobilizing in genomes and function as major drivers of molecular and phenotypic variation [3,4]. Despite their selfish behavior, TEs often contribute to adaptation at individual loci as well as large-scale reshaping of gene regulatory networks resulting in adaptive novelty [3–8]. Furthermore, TEs passively shape the distribution of genomic structural variants (including gene duplications and deletions) due to their tendency to facilitate nonallelic homologous recombination (NAHR) as well as their susceptibility to double stranded breaks during replication, with TE-rich genomic regions displaying a greater propensity for structural variation than TE-poor regions [9–15] (**Figure 1A**). TEs are non-randomly distributed across many genomes, and often show massive enrichment in specific compartments [5,16–19]. Although TE-rich compartments are usually depleted in genes likely due to the deleterious effects of TE-associated variation, some genes show enrichment for these regions [16,20–22]. This "TE compartmentalization" of specific genes may arise as a consequence of direct selection on TEs that generate adaptive variation or passively when TEs create the preconditions necessary for adaptive structural rearrangements [5,6,17,20,23–27]. Here, we show consistent patterns of TE compartmentalization across 1.7 billion years of eukaryotic evolution. This implies that natural selection can drive emergent broad-scale properties of genome architecture.

TEs colocalize with multigene families involved in specific functions

We developed a pipeline to search for patterns of colocalization between transposable elements and gene families involved in specific functions across diverse eukaryotes. To do this, we first generated *de novo* TE libraries and annotations as well as genome-specific gene ontology (GO) databases for 514 annotated genomes available through Refseq or Genbank (Supplemental Table S1; see methods). We performed extensive systematic and manual filtering for genome and GO database quality, resulting in a final set of 325 genomes (Supplemental Table S2). Then, for each species we extracted the 50 kb flanking regions of each gene and identified genes whose flanks displayed the top 90th percentile of TE content, which we refer to as "TE-compartmentalized genes" (see methods). We searched for commonalities among TE-compartmentalized genes using GO enrichment tests (Supplemental Data S1; Supplemental Tables S3-6). Due to massive variation in GO annotation extent and quality across considered species, with genes in some species showing annotations as specific as "evasion of host immune system" and others showing more general annotations such as "protein binding" or "membrane", we also conducted extensive literature reviews to illuminate patterns from less specific annotations (Supplemental Data S1).

Our results reveal consistent patterns of enrichment for multigene families involved in specific functions across 1.7 billion years of eukaryotic evolution notwithstanding massive variation in TE content (Figure 1B-C). In nonpathogenic species, TE-compartmentalized genes include those

involved in sensory perception, environmental interaction and defense, whereas for pathogenic species, genes include those involved in pathogenicity. Furthermore, TE-compartmentalized genes are enriched for multigene families, with ~80% of considered species showing as much as a 20 fold increase in gene family representation (genes with >9 homologs) within TE-compartmentalized genes compared to other genes (Binomial test, $P<0.000001$; Figure 1D; Supplemental Tables S7-8). Remarkably, these patterns persist despite the lack of broad-scale synteny [28,29], multiple independent origins of gene families and functions [30], and vastly different repeat landscapes across divergent eukaryotes [3] (Figure 1C, E-H).

We hypothesize that these and other shared patterns reflect a combination of direct and indirect selection on TE-associated variation affecting genes under strong positive selective pressures. Specifically, TE insertions alter regulatory landscapes of neighboring genes (*e.g.,* by introducing enhancer binding sites or triggering host-mediated silencing). Additionally, TEs facilitate genomic structural rearrangements resulting in new gene duplications and deletions.

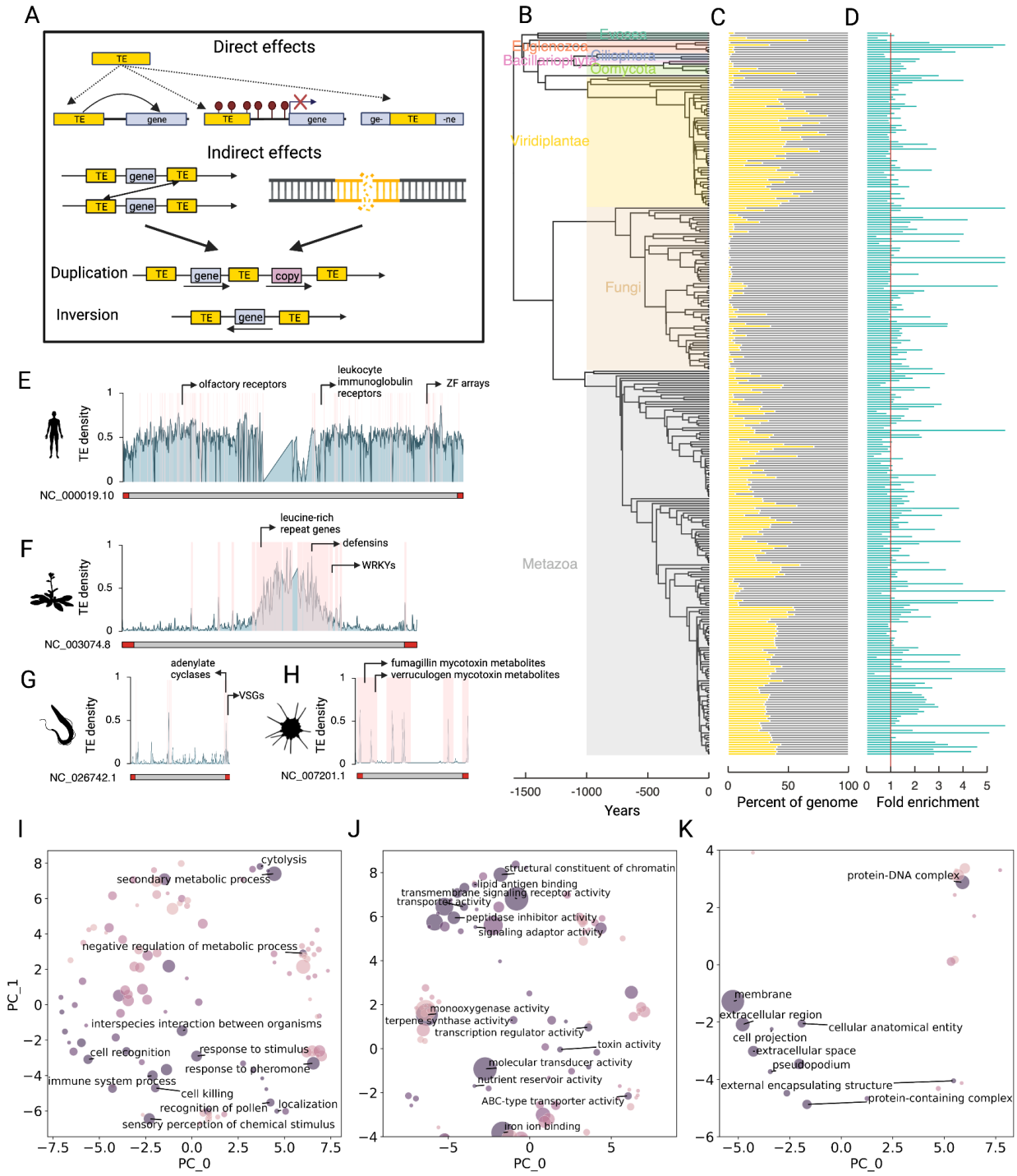

Figure 1: (**A**) Mutational effects of TEs. TEs can facilitate ectopic recombination and double stranded breaks resulting in genomic structural rearrangements such as duplications or inversions. TEs can also affect gene expression by distributing regulatory elements or altering heterochromatin environments. **(B)** Phylogeny of surveyed eukaryotic species. Branch lengths in millions of years were obtained from Timetree [31]. (**C**) Barcharts show proportions of the genome occupied by TEs for each species. **(D)** Fold enrichment of TE-compartmentalized genes for

multigene families. Values above the red line (placed at one) enriched. **(E-H)** Ideograms displaying TE density for (**E**) *Homo sapiens* chromosome 9 (Refseq NC_000019.10), (**F**) *Arabidopsis thaliana* chromosome 3 (Refseq NC_003074.8), (**G**) chromosome 9 of the trypanosome parasite, *Trypanasoma brucei* (Refseq NC_0267642.1), and **(H)** chromosome 8 of the pathogenic fungi, *Aspergillus fumigatus* (Refseq NC_007201.1) across 50 kb windows. TE-compartmentalized gene positions are highlighted in pink and the respective genomic positions of selected TE-compartmentalized gene families are labeled for each species. Red segments at the ends of chromosomes denote subtelomeric regions. (**I-K**) Multidimensional scaling results for enriched (**I**) Biological Process, (**J**) Molecular Function and (**K**) Cellular Component gene ontology (GO) terms for TE-compartmentalized genes across all surveyed species (Supplemental Tables S9-11). Each point represents a GO term, and point size and color correspond to enrichment frequency across species. Terms with dispensability metrics less than 0.007, 0.03 and 0.02 are labeled for Biological Process, Molecular Function and Cellular Component respectively to prevent overcrowding.

Enrichment for genes involved in sensory perception, environmental interaction, defense and pathogenicity

Our survey demonstrates remarkable patterns of enrichment for TE-compartmentalized genes involved in sensory perception, environmental interaction, pathogenicity and defense across the eukaryotic tree of life. This signal remains even when we aggregate our results across this exceptional diversity. Dimensionality reduction on aggregated enriched GO terms for "Biological Processes" reveals the strongest patterns for terms such as "immune system process", "response to stimulus", "interspecies interaction between organisms", "cell killing" and "secondary metabolism" (Figure 1I, Dispensability < 0.007). Similarly, abundantly enriched "Molecular Functions" include "transmembrane signaling receptor activity", "toxin activity" and "antigen binding" (Figure 1J, Dispensability <0.03). "Cellular Component" results generally reflect these patterns, showing enrichment for terms broadly associated with environmental interaction, such as "extracellular space" (Figure 1K, Dispensability <0.02).

Sensory perception and environmental interaction

TE-compartmentalized genes show enrichment for sensory perception and environmental interaction. In metazoans, G protein-coupled receptors are enriched in species spanning from mouse (*Mus musculus*) to placozoans (*Trichoplax adhaerens*). GCPRs such as olfactory receptors represent some of the largest gene families in metazoans, play important roles in sensory perception and evolve rapidly in copy number due to positive selection (Figure 1E; Supplemental Table S5-6) [32–34]. Primarily sessile organisms such as land plants and fungi, and single cell organisms such as red algae secrete secondary metabolites to interact with their environments [35,36]. Like GCPRs, genes involved in secondary metabolism and extracellular interactions are large gene families that evolve adaptively [37–43]. In *Arabidopsis thaliana* for example, TE-compartmentalized genes include for WRKY transcription factors, which play important roles in response to abiotic and biotic stresses and show patterns of rapid expansion and diversification across plant species (Figure 1F) [44]. More broadly, genes involved in

secondary metabolic processes and/or extracellular interactions are enriched in ~62-75% of surveyed land plants and fungi (Figures 1I-K; Supplemental Tables S5-6).

Defense

TE-compartmentalized genes also show enrichment for functions involved in defense in diverse eukaryotes. In the human genome, we observe enrichment for MHC complex genes as well as arrays of killer cell and leukocyte immunoglobulin receptors (Figure 1E). These innate and adaptive immunity genes are also among the most rapidly evolving genes in metazoans due to strong selective pressures from competing pathogens [45–50]. More broadly, 70% of chordates show enrichment for "MHC complex" genes and genes involved in "antigen binding" (Supplemental Data S1; Supplemental Tables S5-6). We observe similar patterns for zinc finger (ZF) genes in metazoans, despite their poor annotation in most genomes (Figure 1E). ZFs are the most abundant transcription factors in metazoans and evolve rapidly under strong selective pressure due important for host defense against transposable elements (Figure 1E) [51]. In plants such as *Arabadopsis thaliana*, we also find vital gene families for plant defense such as RING protein genes, leucine-rich repeat genes, and defensins, consistent with previous reports (Figure 1F) [5,17,52,53]. Consistent with observed trends for chordates, over 70% of land plants show enrichment for "defense response to fungus" and "killing cells of other organism" in addition to other terms clearly related to defense (Supplemental Data S1; Supplemental Tables S5-6).

Pathogenicity

Pathogens frequently exhibit rapidly evolving "accessory genomes," which harbor important gene families for pathogenesis and host adaptation. In the "two-speed" genomes of some fungal and oomycete plant pathogens, TEs colocalize with these gene families and play important roles in driving their dynamic evolution under positive selection [5,54,55]. Our pipeline recovers expected patterns for species with known "two-speed" genome architectures, such as the potato blight-causing *Phytophthora infestans*, in which TE-compartmentalized genes are enriched for terms such as "host intracellular part" (Supplemental Table S4) [56]. However, our results reveal similar trends in additional diverse pathogens. These include the trypanosome human parasite, *Trypanasoma brucei*, and the fungal human pathogen, *Aspergillus fumigatus*.
TE-compartmentalized genes in *T. brucei* show enrichment for functional terms like "evasion of host immune response" and include variant surface glycoproteins and adenylate cyclases crucial for evasion of host immune response (Figure 1G; Supplemental Table S4) [57–60]. In *A. fumigatus*, TE-compartmentalized include all annotated genes involved in verruculogen and fumagillin metabolism, mycotoxins linked to pathogenicity (Figure 1H; Supplemental Table S3-4) [61,62]. Gene ontology terms clearly related to host interactions and pathogenicity are poorly annotated for many species. Nonetheless, many pathogens show enrichment for extracellularly secreted gene products as well as various enzymes and biosynthesis processes, as revealed by manual inspection [5,19,63–66].

TE-compartmentalized gene families show molecular signatures of positive selection

We hypothesized that TE-compartmentalized gene families should show evidence for strong positive selection at the nucleotide level, as reported for a subset of lineages where dynamic gene family evolution is associated with TEs [5,39,40,66–72]. To evaluate this prediction across eukaryotes, we tested for molecular signatures of positive selection for all gene families with at least 10 genes in each considered species (Supplemental Data S2; see methods). TE-compartmentalized gene families show an increased proportion of sites with signatures of positive selection compared to other genes (P(positive selection) > .95; Figure 2A, two-way binomial test, P< 0.001; Supplemental Table S12). Importantly, TE-compartmentalized gene families also show increased proportions of sites with signatures of constraint (P(constraint) > .95; Figure 2B; two-way binomial test, P=0.002; Supplemental Table S12), suggesting that observed patterns of increased TE content for TE-compartmentalized genes cannot be explained merely by relaxed selection [46,73]. Notably, we observe these trends regardless of taxonomic binning, even when highly divergent eukaryotic lineages are analyzed independently, suggesting that species relatedness does not explain these observed patterns. These results suggest that TE-compartmentalized gene families evolve under positive selection.

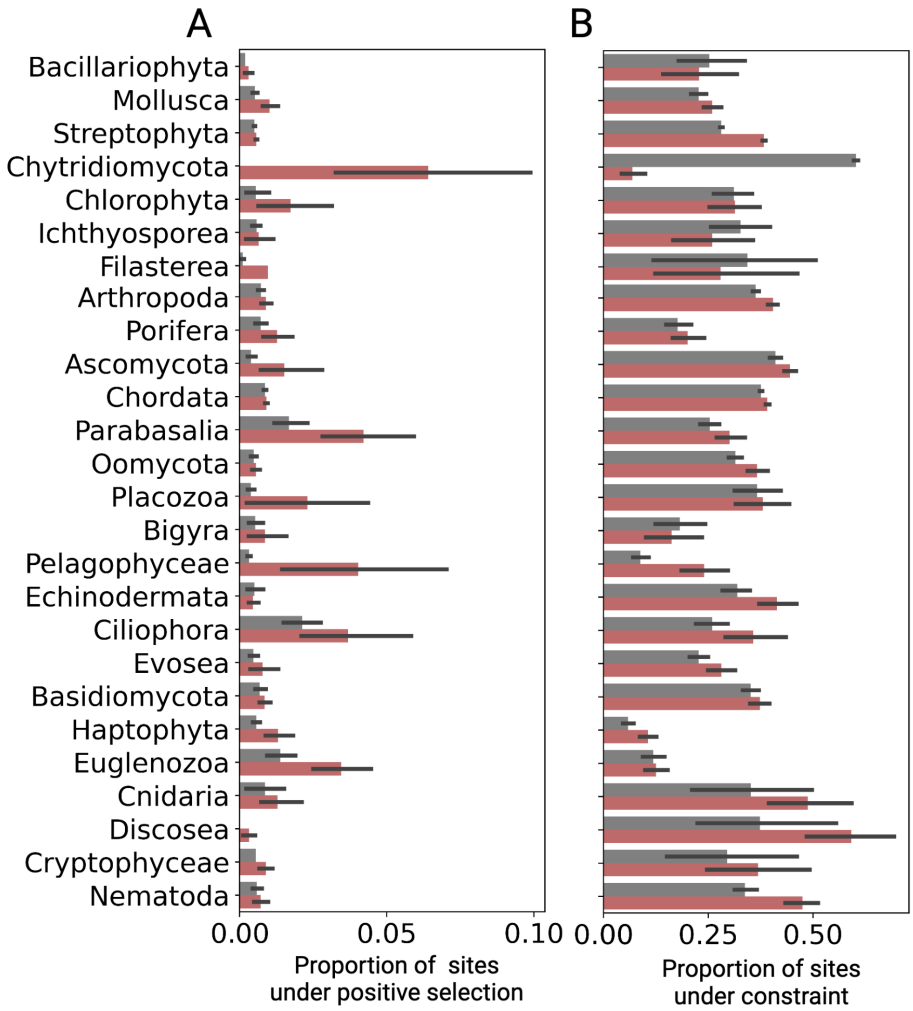

Figure 2: (A-B) Proportion of sites displaying significant signatures of **(A)** positive selection (P(positive selection) > 0.95) and **(B)** selective constraint (P(constraint) > 0.95) for TE-compartmentalized gene families (red) and other gene families (gray) in diverse eukaryotic taxonomic groups. Signatures of selection were predicted using FUBAR [74].

TE-compartmentalized genes show diverse chromosomal distributions

Signatures of genomic compartmentalization are not constrained to specific regions along chromosomes. Genomic distributions of TEs vary tremendously across species, with some chromosomes showing increased TE content in subtelomeric regions and others showing contrasting patterns in which TEs cluster around centromeres [16,54,75]. In many species, TE-compartmentalized genes show a bias towards subtelomeric regions, which are known to undergo frequent structural variation and serve as a cradle of adaptation in several lineages (Supplemental Figure S1; two-way permutation test, alpha = 0.05, N = 1000) [75]. However, in other species we observe the opposite pattern, in which TE-compartmentalized genes are depleted from subtelomeric regions [73], suggesting that TE compartmentalization can arise irrespective of chromosomal position (Supplemental Figure S1). Importantly, we also find little

evidence for consistent trends of association between TE-compartmentalized genes and recombination rates, or TE-compartmentalized genes and GC content, suggesting that these genomic features alone cannot explain observed patterns (two-way binomial test, P=0.064 and P=0.701 respectively; Supplemental Figures S2-S3; see Methods).

Positive selection might contribute to TE compartmentalization in populations

Positive selection might contribute to the origin and maintenance of TE compartmentalization within species. We used publicly available genomic data to analyze patterns of polymorphism in fruit fly (*D. melanogaster*) populations. Specifically, we compared the allele frequency spectrum of TE variants and single nucleotide variants (SNVs) for TE-compartmentalized genes and other genes across 50 long-read based fruit fly genomes (Supplemental Table S13). Interestingly, TE-compartmentalized genes exhibit an excess of high-frequency alleles for TE variants in their flanking regions, but not for SNVs in their coding regions (χ^2 test P<0.001, Figure 3A). In fact, we observe a depletion of high-frequency SNVs in TE-compartmentalized genes compared to other genes (χ^2 test P<0.001, Figure 3B-C). Assuming that most TE insertions around genes are deleterious or neutral, this pattern suggests that selection might favor TE variants around TE-compartmentalized genes. Thus, positive selection might contribute to the evolution of TE compartmentalization.

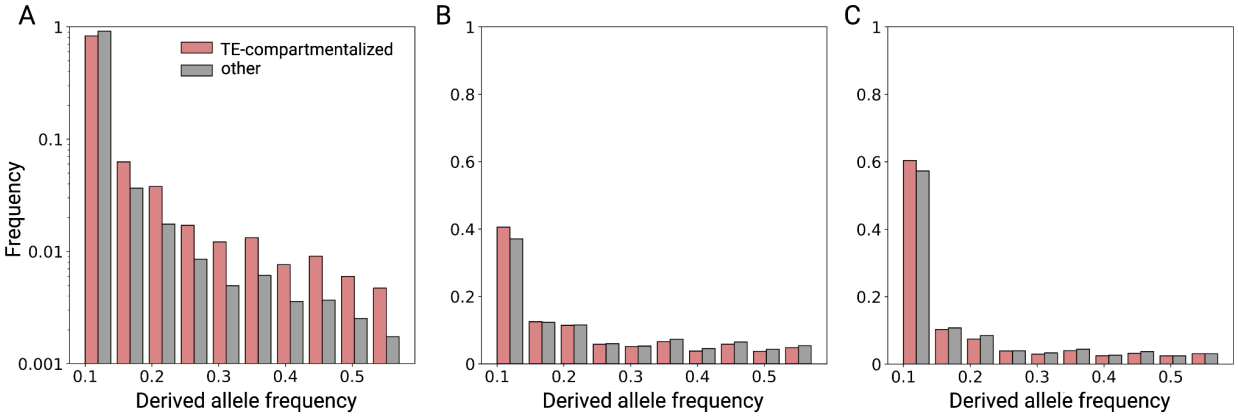

Figure 3: Folded allele frequency spectra for **(A)** TE variants in gene flanking regions, as well as **(B)** synonymous and **(C)** nonsynonymous SNVs in coding regions for TE-compartmentalized genes (red) and other genes (gray).

TEs with the largest predicted mutagenic effects drive compartmentalization signatures in many species

TEs with the largest predicted molecular impacts are the most enriched in repeat hotspots surrounding rapidly evolving gene families. Longer TEs such as long interspersed nuclear elements (LINEs) and long terminal repeat (LTR) retrotransposons are more likely to generate genomic rearrangements and influence gene expression than shorter TEs such as short interspersed nuclear elements (SINEs) [76,77]. We find that LINE-compartmentalized genes and LTR-compartmentalized genes show significantly different functional profiles from

SINE-compartmentalized genes for ~79% and ~76% of enriched functional terms respectively (Supplemental Tables S14-16; see methods). Furthermore, LINEs and LTRs are the main contributors to compartmentalization signatures in species where LINEs, LTRs and SINEs are all present. For example, LINE-compartmentalized genes are enriched for olfactory receptors in 87% of chordates, whereas olfactory receptors are mostly underrepresented in SINE-compartmentalized genes (Supplemental Data S3). Similarly, LINE-compartmentalized genes are enriched for secondary metabolism in all considered ascomycete fungi while SINE-compartmentalized genes are underrepresented for secondary metabolism in 83% of ascomycete species (Supplemental Data S3). Although differences in TE insertional preference could also contribute to these patterns, the enrichment of longer TEs around rapidly evolving gene families is consistent with a model in which selection favors large-affect mutations driving dynamic gene family evolution.

The compartmentalized plasticity model for genome evolution

The origins of eukaryotic genome architecture remain a fundamental question. Theory [23] and empirical analysis [78,79] show that genomes can restructure themselves due to the beneficial effects of genomic structural plasticity, resulting in the colocalization between TEs and gene families for which copy number variation is beneficial. Fungal plant pathogens similarly illuminate extreme examples of TE compartmentalization wherein genomes show bimodal distributions of TE content and TE-rich compartments house genes involved in pathogenicity [5,19,71,80]. Here, we demonstrate remarkable patterns of convergence across eukaryotic lineages spanning 1.7 billion years of evolution, in which TE-compartmentalized genes primarily represent multigene families involved in the same functions and evolve under positive selection. While relaxed purifying selection is a plausible alternative that undoubtedly accounts for some of the excess of TEs observed for TE-compartmentalized genes [17], the lack of evidence for reduced constraint on these genes at the molecular level in diverse lineages as well as the excess of high-frequency derived TE insertions around such genes in fruit fly populations, is consistent with a role for positive selection.

We propose a compartmentalized plasticity model for genome evolution, wherein selection favors the colocalization between TEs and gene families for which rapid evolution is advantageous (Figure 4). Specifically, while TEs likely to impact gene expression or genome stability are generally depleted around essential genes due to their deleterious effects [17,76,81–84], selection may occasionally favor TE-associated mutations affecting rapidly evolving gene families. Over time, recurrent selective sweeps on TEs and TE-associated structural variants affecting these genes could result in TE compartmentalization. Subsequent TE compartmentalization functions as a positive feedback loop, promoting higher rates of variation and potential adaptive novelty for these gene families. These results illuminate a major universal feature of eukaryotic genome evolution.

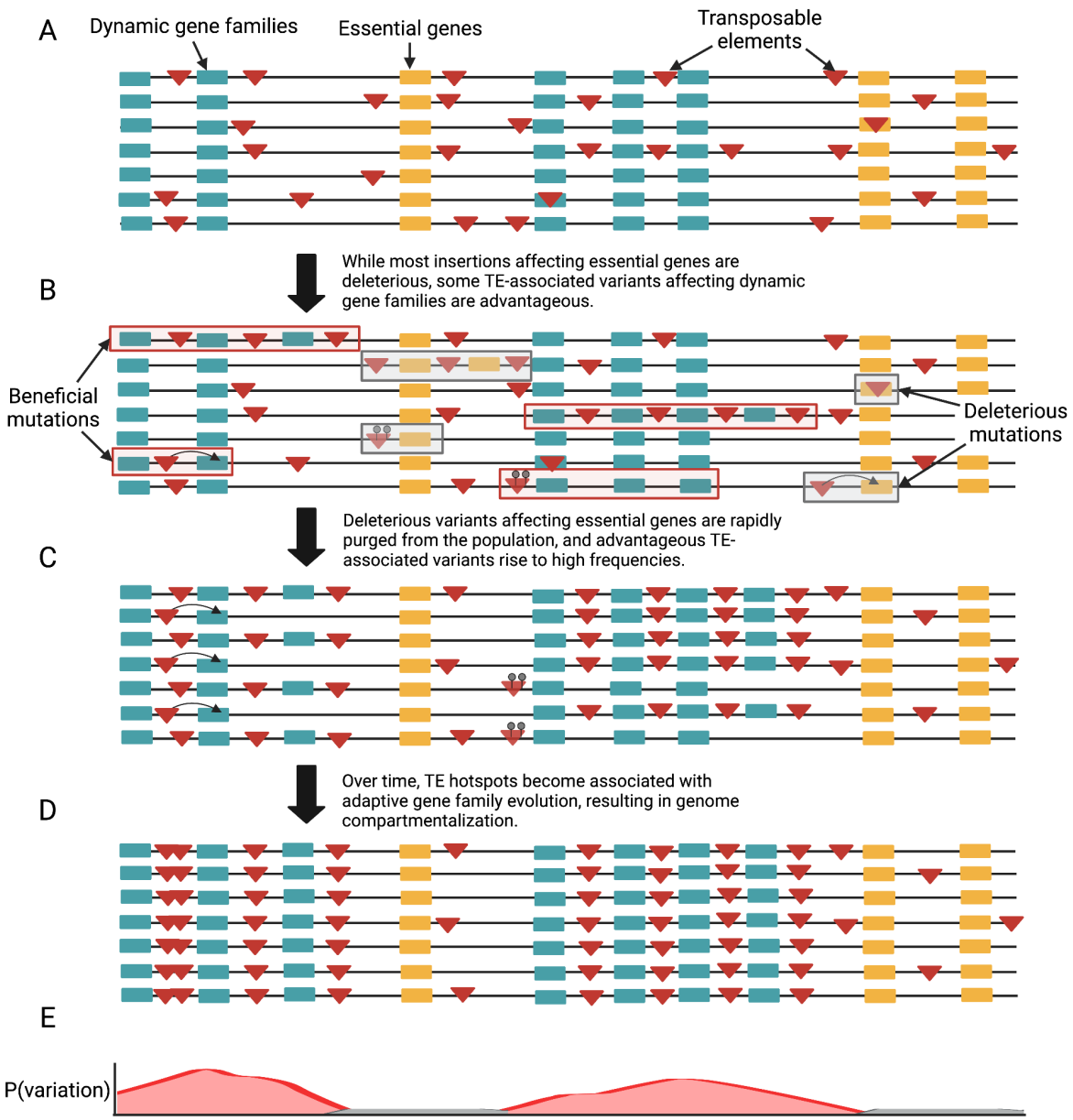

Figure 4: Compartmentalized plasticity model for genome evolution. Each line represents a haplotype within a population. Green boxes and yellow boxes delineate labile genes and essential genes respectively. Transposable elements are shown as red triangles. (**A**) Transposable elements insert semi-randomly across the genome. (**B**) Most TE insertions affecting essential genes (gray boxes) are deleterious. Some TE-associated variants affecting dynamic genes (red boxes) are advantageous. (**C**) Deleterious variants are rapidly purged from the population, whereas advantageous variants rise to high frequencies. (**D**) Over time labile genes colocalize with TEs, forming TE-rich compartments. (**E**) This colocalization functions as a positive feedback loop, since TE-compartmentalized genes exhibit an increased probability for future TE insertions and associated structural and regulatory variation.

Methods

Retrieving relevant genomic data

We downloaded all considered genome assemblies and annotations from NCBI [85] (Accessed February 20, 2020). We only considered genomes with RefSeq [86] assemblies for quality control purposes. However, we opted to use GenBank [85] assemblies and annotations for species in which GenBank annotations exhibit superior gene function annotations. We downloaded functional annotations for each species from Uniprot [87]. Accessions and metadata for all genomes used for the TE compartmentalization survey are displayed in Supplemental Table S1. We also downloaded additional *D. melanogaster* genomes from genbank for population analyses, listed in Supplemental Table S13. Code for our TE compartmentalization pipeline is available on github (https://github.com/lgozasht/TE-compartmentalization).

Repeat mining and annotation

To analyze patterns of repeat distributions across species, we first annotated transposable elements in each considered genome. We employed RepeatModeler (version 2.0.2) [88] to generate species-specific TE libraries *de novo* for each genome. Then, we processed each library to remove high copy number genes not associated with transposable elements. To do this, we used BLAST [89] to identify homologous sequences between candidate TEs and each genome's transcript library as well as TE-related genes available from RepeatMasker. Then, we removed candidate TEs displaying strong homology (e-value < 1e-25) to species transcripts, ignoring those which showed homology to known TE genes. We used RepeatMasker (version 4.1.2) [88] to annotate TEs and simple repeats in each genome using each respective *de novo* repeat library as input, with the flags *-s -no_is -u -noisy -html -xm -a -xsmall* and resolved overlapping annotations using RM2Bed.py (https://github.com/rmhubley/RepeatMasker/blob/master/util/RM2Bed.py) with the *-o higher_score* flag. All TE libraries are being deposited to the DFAM database [90].

Identifying TE-compartmentalized genes

To identify TE-compartmentalized genes, for each species we first extracted the 50 kb flanking regions for each gene using bedtools (version 2.29.1) flank [91]. We then intersected these regions with all protein coding genes using bedtools intersect and filtered out flanking regions which overlapped other protein coding genes. We used bedtools coverage and species-specific TE annotations to calculate TE density for the flanking regions of each gene. We define TE density as the proportion of bases occupied by TEs for a given region. We define TE-compartmentalized genes as genes within the top 90th percentile of TE density when the full distribution of gene TE densities is considered independently for each species. We note that we explored multiple cutoffs for TE compartmentalization including 85th, 95th and 99th percentile cutoffs, as well as different flanking region lengths (e.g. 10kb) and achieved similar results. We also computed TE-compartmentalized genes separately for all TEs, LINEs, SINEs, LTR retrotransposons, and DNA transposons.

Gene ontology database construction, analysis and filtering

We constructed species specific gene ontology (GO) databases for each genome. To do this, we extracted all gene ontology annotations corresponding to annotated genes in each genome from Uniprot [87] as well as AmiGo [92]. Then, for each species, we filtered our gene set to only include genes with GO annotations. We performed GO enrichment tests for TE-compartmentalized genes using goatools [93] with the flag *--method fdr_bh*. Goatools performes GO enrichment tests using a fisher's exact tests with a false discovery correction. We required a minimum of four genes in test sets and filtered out species for which less than 20% of genes possessed GO annotations, resulting in the removal of 118 species. Furthermore, after performing GO enrichment and purification (underrepresentation) tests for TE-compartmentalized genes in each species, we found that species which displayed no significant enrichment or purification results had significantly smaller GO databases than species with significant results (two-way ManwhitneyU test, $P<0.0001$). In light of this, we reasoned that our inability to find patterns of functional enrichment was likely due to poor GO annotation quality and/or lack of power in these species. Consistent with this, for species where we observed no fdr corrected significance, the top 5 most enriched terms with P values <0.05 showed consistent congruence with trends of term enrichment for species where we achieve fdr corrected significance. Thus, we considered these results in our downstream analyses. However, we filtered another 69 species which displayed no functional enrichment results with $P<0.05$. Together, after these filters, we were left with 325 species (Supplemental Table S2). To make sense of this complex dataset, we performed multidimensional scaling using a matrix of GO term semantic similarities through REVIGO, merging terms with dispensability > 0.5 [94]. This reduced redundancy in our dataset and also provided metrics and a systematic framework with which to identify the most enriched terms and abundant terms. In our case, the dispensability metric is calculated based on both semantic relatedness to other terms and enrichment frequency. Figure 1B-D was produced using REVIGO output, with "Biological Process," "Molecular Function" and "Cellular Component" terms labeled using dispensability cutoff of less than 0.007, 0.03 and 0.02 respectively.

Testing for molecular signatures of selection across gene families

We downloaded corresponding transcriptome fasta files from Refseq or Genbank for each considered species, and extracted the longest transcript for each coding gene in each genome. Then, we used a variation of the *FUSTr* pipeline [95] to cluster gene families and test for molecular signatures of positive selection. The *FUSTr* pipeline was developed for transcriptome data, and the primary purpose of the first four steps of the pipeline is transcriptome input processing. Thus, we skipped these steps. Briefly, the remaining steps of the pipeline are as follows. First, *FUSTr* performs an all-by-all blast between proteins using *diamond* [96] and clusters gene families using *silixx* [97]. Then, *FUSTr* generates a multiple sequence alignment for each gene family using *MAFFT* [98] and a subsequent phylogeny using *fasttree* [99] as well as a trimmed alignment using *trimal* [100] for input to *FUBAR* [74], which performs tests for positive and negative selection at the

molecular level. For downstream analyses and producing Figure 2, we required that each species have at least one TE-compartmentalized gene family and at least one non-TE-compartmentalized gene family.

Genomic signature and chromosomal distribution analysis

Since GC-content can also contribute to differences in gene content as well as TE content within genomes, we also tested for differences in GC content between TE-compartmentalized genes and other genes across phyla. We separately calculated GC content for all genes as well as 50kb of noncoding sequence flanking genes using bedtools nuc [91]. Although some individual eukaryotic lineages displayed differences in genic and/or gene-flanking GC content between TE-compartmentalized genes and other genes, we found very little evidence for any trend across diverse lineages (Supplemental Figure S2; two-way Binomial test, P=0.701). Recombination rates often correlate with TE distributions [101], and TEs can accumulate in regions of low recombination due to reduced efficacy of selection in such regions as well as selection against ectopic recombination in highly recombining regions [102]. Thus, it is conceivable that reduced recombination rates for TE-compartmentalized genes could explain observed patterns To evaluate this possibility, we intersected our TE compartmentalization results with recombination data for a subset of species (retrieved from [103]). Specifically, we compared recombination rates for regions containing TE-compartmentalized genes to regions containing other genes. We find no significant trend of reduced recombination rates for TE-compartmentalized genes (Supplemental Figure S3; two-way Binomial test, P=0.064). Furthermore, for species in which TE-compartmentalized genes exhibit reduced recombination rates overall, we still observe outliers which display increased recombination rates relative to the median recombination rate for non-TE-compartmentalized genes (Supplemental Figure S3). Together, these results suggest that although recombination rates undoubtedly affects TE distributions, recombination rates alone fail to explain observed patterns

We explored chromosomal distributions of TE-compartmentalized genes for genomes with chromosome level assemblies. Specifically, we were interested in testing for enrichment or depletion of TE-compartmentalized genes at the ends of chromosomes (in prospective subtelomeric regions). Given the diversity of species considered in our study, we crudely assigned subtelomeric regions based on chromosome size, using the first 10% and last 10% of bases on a given chromosome. Then, for each chromosome in each species, we compared observed proportions of TE-compartmentalized genes in these regions to expectations from random resampling across 1000 permutations.

Population genetic analysis

We aligned 50 long-read based *D. melanogaster* genome assemblies to the *D. melanogaster* RefSeq assembly using minmap2 (version 2.21-r1071) with parameters *-a --eqx -x asm20 --cs -r2k -t 9* [104]. Then, we used samtools (version 1.11) to convert alignments in sam format to sorted

bam files [105]. We employed svim-asm (version 1.0.3) with parameters *haploid --max_sv_size 100000000* to call genomic structural variants, SNPs and indels for each genome [106]. We merged structural variant calls from each genome into one call set using SURVIVOR [107] with the parameters 500 1 1 1 0 50, which combines prospective redundant SV calls based on breakpoint vicinity (if both breakpoints are within 500 bp of each other) and filters for SVs longer than 50 bp. We extracted sequences for insertions and deletions, removed those which mostly contained ambiguous nucleotides, and ran Repeatmasker on them using our *D. melanogaster* TE library to identify TE-associated SVs. Finally, we filtered our structural variant callset for insertions or deletions which displayed at least 50% coverage for a TE. For SNPs and indels, we filtered for biallelic variants and merged calls for each genome using Bcftools (version 1.9) merge and Bcftools view respectively [108]. We annotated synonymous and nonsynonymous variants with SnpEff (version 5.1d) [109]. Population genetic analyses were performed using scikit-allel (version 1.3.3) (https://zenodo.org/badge/latestdoi/7890/cggh/scikit-allel).

Comparing compartmentalization signatures between LTRs, LINEs and SINEs

We performed Fisher's Exact Tests comparing proportions of TE-compartmentalized genes corresponding to each gene ontology term across all considered species between all combinations of LTR-compartmentalized genes, LINE-compartmentalized genes, and SINE-compartmentalized genes (Supplemental Tables S14-16). We used FDR corrected Q values to assess the proportion of terms with significantly different results for each combination of TE classes. This revealed that LINE-compartmentalized and LTR-compartmentalized genes showed significantly different enrichment results for only ~28% of terms, whereas each significantly differed from SINE compartmentalized genes for >75% of terms. Since many GO terms are challenging to compare over long evolutionary distances, we also conducted these tests independently for different clades.

Acknowledgements

The authors thank Daniel Hartl, Cedric Feschotte, Sean Eddy, Tom Jones, Jenny Chen, Andreas Kautt, Matthew Hahn, James Mallet, Magnus Norborg and Timothy B. Sackton for helpful discussions and feedback on this manuscript. L. G. thanks Hopi Hoekstra for her support and advice throughout this work. The computations for this work were run on the FASRC Cannon cluster supported by the FAS Division of Science Research Computing Group at Harvard University.

References

1. Gozashti, L. *et al.* Transposable elements drive intron gain in diverse eukaryotes. *Proc. Natl. Acad. Sci. U. S. A.* **119**, e2209766119 (2022).

2. Fernández, R. & Gabaldón, T. Gene gain and loss across the metazoan tree of life. *Nat Ecol*

Evol **4**, 524–533 (2020).

3. Wells, J. N. & Feschotte, C. A Field Guide to Eukaryotic Transposable Elements. *Annu. Rev. Genet.* **54**, 539–561 (2020).

4. Bourque, G. *et al.* Ten things you should know about transposable elements. *Genome Biol.* **19**, 199 (2018).

5. Seidl, M. F. & Thomma, B. P. H. J. Transposable Elements Direct The Coevolution between Plants and Microbes. *Trends Genet.* **33**, 842–851 (2017).

6. Schrader, L. & Schmitz, J. The impact of transposable elements in adaptive evolution. *Mol. Ecol.* **28**, 1537–1549 (2019).

7. Stapley, J., Santure, A. W. & Dennis, S. R. Transposable elements as agents of rapid adaptation may explain the genetic paradox of invasive species. *Mol. Ecol.* **24**, 2241–2252 (2015).

8. Ellison, C. E. & Bachtrog, D. Dosage compensation via transposable element mediated rewiring of a regulatory network. *Science* **342**, 846–850 (2013).

9. Montgomery, E. A., Huang, S. M., Langley, C. H. & Judd, B. H. Chromosome rearrangement by ectopic recombination in Drosophila melanogaster: genome structure and evolution. *Genetics* **129**, 1085–1098 (1991).

10. Weckselblatt, B. & Rudd, M. K. Human Structural Variation: Mechanisms of Chromosome Rearrangements. *Trends Genet.* **31**, 587–599 (2015).

11. Wicker, T., Buchmann, J. P. & Keller, B. Patching gaps in plant genomes results in gene movement and erosion of colinearity. *Genome Res.* **20**, 1229–1237 (2010).

12. Lambert, S., Watson, A., Sheedy, D. M., Martin, B. & Carr, A. M. Gross chromosomal rearrangements and elevated recombination at an inducible site-specific replication fork barrier. *Cell* **121**, 689–702 (2005).

13. Cáceres, M., Puig, M. & Ruiz, A. Molecular characterization of two natural hotspots in the Drosophila buzzatii genome induced by transposon insertions. *Genome Res.* **11**, 1353–1364 (2001).

14. Voineagu, I., Narayanan, V., Lobachev, K. S. & Mirkin, S. M. Replication stalling at unstable inverted repeats: interplay between DNA hairpins and fork stabilizing proteins. *Proc. Natl. Acad. Sci. U. S. A.* **105**, 9936–9941 (2008).

15. Lobachev, K. S. *et al.* Inverted Alu repeats unstable in yeast are excluded from the human genome. *EMBO J.* **19**, 3822–3830 (2000).

16. Wright, S. I., Agrawal, N. & Bureau, T. E. Effects of recombination rate and gene density on transposable element distributions in Arabidopsis thaliana. *Genome Res.* **13**, 1897–1903 (2003).

17. Quadrana, L. *et al.* The Arabidopsis thaliana mobilome and its impact at the species level.

Elife **5**, (2016).

18. Fan, C. *et al.* The subtelomere of Oryza sativa chromosome 3 short arm as a hot bed of new gene origination in rice. *Mol. Plant* **1**, 839–850 (2008).

19. Wacker, T. *et al.* Two-speed genome evolution drives pathogenicity in fungal pathogens of animals. *Proc. Natl. Acad. Sci. U. S. A.* **120**, e2212633120 (2023).

20. Schrader, L. *et al.* Transposable element islands facilitate adaptation to novel environments in an invasive species. *Nat. Commun.* **5**, 5495 (2014).

21. Bartolomé, C., Maside, X. & Charlesworth, B. On the abundance and distribution of transposable elements in the genome of Drosophila melanogaster. *Mol. Biol. Evol.* **19**, 926–937 (2002).

22. Gozashti, L., Feschotte, C. & Hoekstra, H. E. Transposable Element Interactions Shape the Ecology of the Deer Mouse Genome. *Mol. Biol. Evol.* **40**, (2023).

23. Crombach, A. & Hogeweg, P. Chromosome rearrangements and the evolution of genome structuring and adaptability. *Mol. Biol. Evol.* **24**, 1130–1139 (2007).

24. Išerić, H., Alkan, C., Hach, F. & Numanagić, I. Fast characterization of segmental duplication structure in multiple genome assemblies. *Algorithms Mol. Biol.* **17**, 4 (2022).

25. Fambrini, M., Usai, G., Vangelisti, A., Mascagni, F. & Pugliesi, C. The plastic genome: The impact of transposable elements on gene functionality and genomic structural variations. *Genesis* **58**, e23399 (2020).

26. Correa, M. *et al.* The Transposable Element Environment of Human Genes Differs According to Their Duplication Status and Essentiality. *Genome Biol. Evol.* **13**, (2021).

27. Zhang, P. *et al.* Extrachromosomal circular DNA and structural variants highlight genome instability in Arabidopsis epigenetic mutants. *Nat. Commun.* **14**, 5236 (2023).

28. DeBarry, J. D. & Kissinger, J. C. Jumbled genomes: missing Apicomplexan synteny. *Mol. Biol. Evol.* **28**, 2855–2871 (2011).

29. Eichler, E. E. & Sankoff, D. Structural dynamics of eukaryotic chromosome evolution. *Science* **301**, 793–797 (2003).

30. Lespinet, O., Wolf, Y. I., Koonin, E. V. & Aravind, L. The role of lineage-specific gene family expansion in the evolution of eukaryotes. *Genome Res.* **12**, 1048–1059 (2002).

31. Kumar, S., Stecher, G., Suleski, M. & Hedges, S. B. TimeTree: A Resource for Timelines, Timetrees, and Divergence Times. *Mol. Biol. Evol.* **34**, 1812–1819 (2017).

32. Hughes, G. M. *et al.* The Birth and Death of Olfactory Receptor Gene Families in Mammalian Niche Adaptation. *Mol. Biol. Evol.* **35**, 1390–1406 (2018).

33. Niimura, Y. & Nei, M. Comparative evolutionary analysis of olfactory receptor gene clusters between humans and mice. *Gene* **346**, 13–21 (2005).

34. Yohe, L. R., Fabbri, M., Hanson, M. & Bhullar, B.-A. S. Olfactory receptor gene evolution is unusually rapid across Tetrapoda and outpaces chemosensory phenotypic change. *Curr. Zool.* **66**, 505–514 (2020).

35. Keller, N. P. Fungal secondary metabolism: regulation, function and drug discovery. *Nat. Rev. Microbiol.* **17**, 167–180 (2019).

36. Erb, M. & Kliebenstein, D. J. Plant Secondary Metabolites as Defenses, Regulators, and Primary Metabolites: The Blurred Functional Trichotomy. *Plant Physiol.* **184**, 39–52 (2020).

37. Benderoth, M. *et al.* Positive selection driving diversification in plant secondary metabolism. *Proc. Natl. Acad. Sci. U. S. A.* **103**, 9118–9123 (2006).

38. Kliebenstein, D. J., Lambrix, V. M., Reichelt, M., Gershenzon, J. & Mitchell-Olds, T. Gene duplication in the diversification of secondary metabolism: tandem 2-oxoglutarate-dependent dioxygenases control glucosinolate biosynthesis in Arabidopsis. *Plant Cell* **13**, 681–693 (2001).

39. McHale, L. K. *et al.* Structural variants in the soybean genome localize to clusters of biotic stress-response genes. *Plant Physiol.* **159**, 1295–1308 (2012).

40. Zhang, R., Murat, F., Pont, C., Langin, T. & Salse, J. Paleo-evolutionary plasticity of plant disease resistance genes. *BMC Genomics* **15**, 187 (2014).

41. Speed, M. P., Fenton, A., Jones, M. G., Ruxton, G. D. & Brockhurst, M. A. Coevolution can explain defensive secondary metabolite diversity in plants. *New Phytol.* **208**, 1251–1263 (2015).

42. Gluck-Thaler, E. *et al.* The Architecture of Metabolism Maximizes Biosynthetic Diversity in the Largest Class of Fungi. *Mol. Biol. Evol.* **37**, 2838–2856 (2020).

43. Leister, D. Tandem and segmental gene duplication and recombination in the evolution of plant disease resistance genes. *Trends Genet.* **20**, 116–122 (2004).

44. Bakshi, M. & Oelmüller, R. WRKY transcription factors: Jack of many trades in plants. *Plant Signal. Behav.* **9**, e27700 (2014).

45. Roach, J. C. *et al.* The evolution of vertebrate Toll-like receptors. *Proc. Natl. Acad. Sci. U. S. A.* **102**, 9577–9582 (2005).

46. Nei, M., Gu, X. & Sitnikova, T. Evolution by the birth-and-death process in multigene families of the vertebrate immune system. *Proc. Natl. Acad. Sci. U. S. A.* **94**, 7799–7806 (1997).

47. Anzai, T. *et al.* Comparative sequencing of human and chimpanzee MHC class I regions unveils insertions/deletions as the major path to genomic divergence. *Proc. Natl. Acad. Sci. U. S. A.* **100**, 7708–7713 (2003).

48. Bentkowski, P. & Radwan, J. Evolution of major histocompatibility complex gene copy

number. *PLoS Comput. Biol.* **15**, e1007015 (2019).

49. Gokcumen, O. *et al.* Refinement of primate copy number variation hotspots identifies candidate genomic regions evolving under positive selection. *Genome Biol.* **12**, R52 (2011).

50. Laun, K. *et al.* The leukocyte receptor complex in chicken is characterized by massive expansion and diversification of immunoglobulin-like Loci. *PLoS Genet.* **2**, e73 (2006).

51. Wells, J. N. *et al.* Transposable elements drive the evolution of metazoan zinc finger genes. *bioRxiv* 2022.11.29.518450 (2022) doi:10.1101/2022.11.29.518450.

52. Lin, S.-S. *et al.* RING1 E3 ligase localizes to plasma membrane lipid rafts to trigger FB1-induced programmed cell death in Arabidopsis. *Plant J.* **56**, 550–561 (2008).

53. Marino, D., Peeters, N. & Rivas, S. Ubiquitination during plant immune signaling. *Plant Physiol.* **160**, 15–27 (2012).

54. Croll, D. & McDonald, B. A. The accessory genome as a cradle for adaptive evolution in pathogens. *PLoS Pathog.* **8**, e1002608 (2012).

55. Frantzeskakis, L., Kusch, S. & Panstruga, R. The need for speed: compartmentalized genome evolution in filamentous phytopathogens. *Mol. Plant Pathol.* **20**, 3–7 (2019).

56. Haas, B. J. *et al.* Genome sequence and analysis of the Irish potato famine pathogen Phytophthora infestans. *Nature* **461**, 393–398 (2009).

57. Mugnier, M. R., Stebbins, C. E. & Papavasiliou, F. N. Masters of Disguise: Antigenic Variation and the VSG Coat in Trypanosoma brucei. *PLoS Pathog.* **12**, e1005784 (2016).

58. Silva Pereira, S., Jackson, A. P. & Figueiredo, L. M. Evolution of the variant surface glycoprotein family in African trypanosomes. *Trends Parasitol.* **38**, 23–36 (2022).

59. Pinger, J., Chowdhury, S. & Papavasiliou, F. N. Variant surface glycoprotein density defines an immune evasion threshold for African trypanosomes undergoing antigenic variation. *Nat. Commun.* **8**, 828 (2017).

60. Salmon, D. *et al.* Adenylate cyclases of Trypanosoma brucei inhibit the innate immune response of the host. *Science* **337**, 463–466 (2012).

61. Guruceaga, X. *et al.* Fumagillin, a Mycotoxin of Aspergillus fumigatus: Biosynthesis, Biological Activities, Detection, and Applications. *Toxins* **12**, (2019).

62. Khoufache, K. *et al.* Verruculogen associated with Aspergillus fumigatus hyphae and conidia modifies the electrophysiological properties of human nasal epithelial cells. *BMC Microbiol.* **7**, 5 (2007).

63. Moran, G. P., Coleman, D. C. & Sullivan, D. J. Comparative genomics and the evolution of pathogenicity in human pathogenic fungi. *Eukaryot. Cell* **10**, 34–42 (2011).

64. van der Does, H. C. & Rep, M. Virulence genes and the evolution of host specificity in plant-pathogenic fungi. *Mol. Plant. Microbe. Interact.* **20**, 1175–1182 (2007).

65. Li, J. & Zhang, K.-Q. Independent expansion of zincin metalloproteinases in Onygenales fungi may be associated with their pathogenicity. *PLoS One* **9**, e90225 (2014).

66. Grandaubert, J. *et al.* Transposable element-assisted evolution and adaptation to host plant within the Leptosphaeria maculans-Leptosphaeria biglobosa species complex of fungal pathogens. *BMC Genomics* **15**, 891 (2014).

67. Kulski, J. K. *et al.* The evolution of MHC diversity by segmental duplication and transposition of retroelements. *J. Mol. Evol.* **45**, 599–609 (1997).

68. Kulski, J. K., Shiina, T., Anzai, T., Kohara, S. & Inoko, H. Comparative genomic analysis of the MHC: the evolution of class I duplication blocks, diversity and complexity from shark to man. *Immunol. Rev.* **190**, 95–122 (2002).

69. Bopp, S. E. R. *et al.* Mitotic evolution of Plasmodium falciparum shows a stable core genome but recombination in antigen families. *PLoS Genet.* **9**, e1003293 (2013).

70. Claessens, A. *et al.* Generation of antigenic diversity in Plasmodium falciparum by structured rearrangement of Var genes during mitosis. *PLoS Genet.* **10**, e1004812 (2014).

71. Faino, L. *et al.* Transposons passively and actively contribute to evolution of the two-speed genome of a fungal pathogen. *Genome Res.* **26**, 1091–1100 (2016).

72. Torres, D. E., Thomma, B. P. H. J. & Seidl, M. F. Transposable Elements Contribute to Genome Dynamics and Gene Expression Variation in the Fungal Plant Pathogen Verticillium dahliae. *Genome Biol. Evol.* **13**, (2021).

73. Baduel, P., Quadrana, L., Hunter, B., Bomblies, K. & Colot, V. Relaxed purifying selection in autopolyploids drives transposable element over-accumulation which provides variants for local adaptation. *Nat. Commun.* **10**, 5818 (2019).

74. Murrell, B. *et al.* FUBAR: a fast, unconstrained bayesian approximation for inferring selection. *Mol. Biol. Evol.* **30**, 1196–1205 (2013).

75. Mefford, H. C. & Trask, B. J. The complex structure and dynamic evolution of human subtelomeres. *Nat. Rev. Genet.* **3**, 91–102 (2002).

76. Petrov, D. A., Aminetzach, Y. T., Davis, J. C., Bensasson, D. & Hirsh, A. E. Size matters: non-LTR retrotransposable elements and ectopic recombination in Drosophila. *Mol. Biol. Evol.* **20**, 880–892 (2003).

77. Bourgeois, Y., Ruggiero, R. P., Hariyani, I. & Boissinot, S. Disentangling the determinants of transposable elements dynamics in vertebrate genomes using empirical evidences and simulations. *PLoS Genet.* **16**, e1009082 (2020).

78. Dunham, M. J. *et al.* Characteristic genome rearrangements in experimental evolution of *Saccharomyces cerevisiae*. *Proc. Natl. Acad. Sci. U. S. A.* **99**, 16144–16149 (2002).

79. Brown, C. J., Todd, K. M. & Rosenzweig, R. F. Multiple duplications of yeast hexose transport genes in response to selection in a glucose-limited environment. *Mol. Biol. Evol.*

15, 931–942 (1998).

80. Torres, D. E., Oggenfuss, U., Croll, D. & Seidl, M. F. Genome evolution in fungal plant pathogens: looking beyond the two-speed genome model. *Fungal Biol. Rev.* **34**, 136–143 (2020).

81. Campos-Sánchez, R., Cremona, M. A., Pini, A., Chiaromonte, F. & Makova, K. D. Integration and Fixation Preferences of Human and Mouse Endogenous Retroviruses Uncovered with Functional Data Analysis. *PLoS Comput. Biol.* **12**, e1004956 (2016).

82. Kvikstad, E. M. & Makova, K. D. The (r)evolution of SINE versus LINE distributions in primate genomes: sex chromosomes are important. *Genome Res.* **20**, 600–613 (2010).

83. Boissinot, S., Entezam, A. & Furano, A. V. Selection against deleterious LINE-1-containing loci in the human lineage. *Mol. Biol. Evol.* **18**, 926–935 (2001).

84. Simons, C., Pheasant, M., Makunin, I. V. & Mattick, J. S. Transposon-free regions in mammalian genomes. *Genome Res.* **16**, 164–172 (2006).

85. Sayers, E. W. *et al.* Database resources of the national center for biotechnology information. *Nucleic Acids Res.* **50**, D20–D26 (2022).

86. O'Leary, N. A. *et al.* Reference sequence (RefSeq) database at NCBI: current status, taxonomic expansion, and functional annotation. *Nucleic Acids Res.* **44**, D733–45 (2016).

87. UniProt Consortium. UniProt: the universal protein knowledgebase in 2021. *Nucleic Acids Res.* **49**, D480–D489 (2021).

88. Flynn, J. M. *et al.* RepeatModeler2 for automated genomic discovery of transposable element families. *Proc. Natl. Acad. Sci. U. S. A.* **117**, 9451–9457 (2020).

89. Altschul, S. F., Gish, W., Miller, W., Myers, E. W. & Lipman, D. J. Basic local alignment search tool. *J. Mol. Biol.* **215**, 403–410 (1990).

90. Hubley, R. *et al.* The Dfam database of repetitive DNA families. *Nucleic Acids Res.* **44**, D81–9 (2016).

91. Quinlan, A. R. & Hall, I. M. BEDTools: a flexible suite of utilities for comparing genomic features. *Bioinformatics* **26**, 841–842 (2010).

92. Ashburner, M. *et al.* Gene ontology: tool for the unification of biology. The Gene Ontology Consortium. *Nat. Genet.* **25**, 25–29 (2000).

93. Klopfenstein, D. V. *et al.* GOATOOLS: A Python library for Gene Ontology analyses. *Sci. Rep.* **8**, 10872 (2018).

94. Supek, F., Bošnjak, M., Škunca, N. & Šmuc, T. REVIGO summarizes and visualizes long lists of gene ontology terms. *PLoS One* **6**, e21800 (2011).

95. Cole, T. J. & Brewer, M. S. FUSTr: a tool to find gene families under selection in transcriptomes. *PeerJ* **6**, e4234 (2018).

96. Buchfink, B., Xie, C. & Huson, D. H. Fast and sensitive protein alignment using DIAMOND. *Nat. Methods* **12**, 59–60 (2015).

97. Miele, V., Penel, S. & Duret, L. Ultra-fast sequence clustering from similarity networks with SiLiX. *BMC Bioinformatics* **12**, 116 (2011).

98. Katoh, K. & Standley, D. M. MAFFT Multiple Sequence Alignment Software Version 7: Improvements in Performance and Usability. *Mol. Biol. Evol.* **30**, 772–780 (2013).

99. Price, M. N., Dehal, P. S. & Arkin, A. P. FastTree 2--approximately maximum-likelihood trees for large alignments. *PLoS One* **5**, e9490 (2010).

100. Capella-Gutiérrez, S., Silla-Martínez, J. M. & Gabaldón, T. trimAl: a tool for automated alignment trimming in large-scale phylogenetic analyses. *Bioinformatics* **25**, 1972–1973 (2009).

101. Kent, T. V., Uzunović, J. & Wright, S. I. Coevolution between transposable elements and recombination. *Philos. Trans. R. Soc. Lond. B Biol. Sci.* **372**, (2017).

102. Rizzon, C., Marais, G., Gouy, M. & Biémont, C. Recombination rate and the distribution of transposable elements in the Drosophila melanogaster genome. *Genome Res.* **12**, 400–407 (2002).

103. Corbett-Detig, R. B., Hartl, D. L. & Sackton, T. B. Natural selection constrains neutral diversity across a wide range of species. *PLoS Biol.* **13**, e1002112 (2015).

104. Li, H. Minimap2: pairwise alignment for nucleotide sequences. *Bioinformatics* **34**, 3094–3100 (2018).

105. Li, H. *et al.* The Sequence Alignment/Map format and SAMtools. *Bioinformatics* **25**, 2078–2079 (2009).

106. Heller, D. & Vingron, M. SVIM-asm: structural variant detection from haploid and diploid genome assemblies. *Bioinformatics* **36**, 5519–5521 (2021).

107. Jeffares, D. C. *et al.* Transient structural variations have strong effects on quantitative traits and reproductive isolation in fission yeast. *Nat. Commun.* **8**, 14061 (2017).

108. Danecek, P. *et al.* Twelve years of SAMtools and BCFtools. *Gigascience* **10**, (2021).

109. Cingolani, P. *et al.* A program for annotating and predicting the effects of single nucleotide polymorphisms, SnpEff: SNPs in the genome of Drosophila melanogaster strain w1118; iso-2; iso-3. *Fly* **6**, 80–92 (2012).